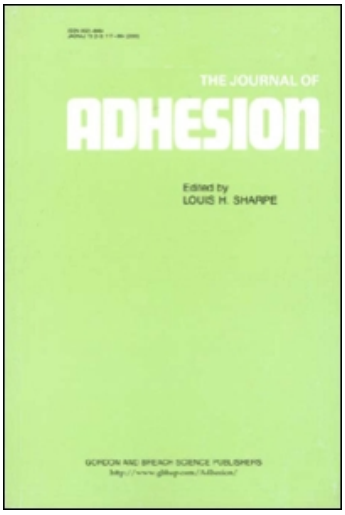


**The Journal of Adhesion**
Publication details, including instructions for authors and subscription information:
http://www.informaworld.com/smpp/title~content=t713453635

# Interfaces in Carbon Fiber/PyrolyticCarbon Matrix Composites

B. L. Butler[a]; D. A. Northrop[a]; T. R. Guess[a]
[a] Composites Research and Development Department, Sandia Laboratories, Albuquerque, New Mexico, U.S.A.

**To cite this Article** Butler, B. L. , Northrop, D. A. and Guess, T. R.(1973) 'Interfaces in Carbon Fiber/PyrolyticCarbon Matrix Composites', The Journal of Adhesion, 5: 2, 161 — 178
**To link to this Article: DOI:** 10.1080/00218467308075018
**URL:** http://dx.doi.org/10.1080/00218467308075018

*J. Adhesion*, 1973, Vol. 5, pp. 161–178

Printed in Northern Ireland

# Interfaces in Carbon Fiber/Pyrolytic-Carbon Matrix Composites†‡

B. L. BUTLER, D. A. NORTHROP and T. R. GUESS

*Composites Research and Development Department, Sandia Laboratories, Albuquerque, New Mexico 87115, U.S.A.*

(*Received January 8, 1973*)



Carbon fiber/pyrolytic-carbon matrix composites contain both fiber-matrix and matrixe matrix interfaces and, thus, do not fit the usual concept of fiber-reinforced composit-materials. This is a consequence of the chemical vapor deposition (CVD) process ir which the matrix forms uniform pyrocarbon sheaths around each fiber and ultimately results in matrix-matrix interfaces with various geometries and also produces large oriented voids. The role of the fiber-matrix and matrix-matrix interfaces on the mechanical composite properties has been examined by mechanical testing and optical and scanning electron microscopy.

Results will be presented for increasingly complex fibrous substrate geometries with a pyrolytic carbon matrix: single fiber, strand or yarn bundle and circumferential and angle-ply filament-wound cylinders. Data for coated single fibers demonstrate the adequacy of the fiber-matrix interface and the applicability of the rule-of-mixtures to this simple composite. The degree of utilization of these coated fiber units in composite structures, however, is determined by the geometry and strength of the matrix-matrix interface, which in turn, is influenced by the microstructure and properties of the pyrolytic carbon. Observed strengths of unidirectional, infiltrated strands are significantly lower than the strengths of the coated single fiber units of which they are composed. This is because the brittle matrix-matrix interfaces are unable to distribute the load equally between the fiber-matrix units or to redistribute the load around individual unit failures. Attempts to predict strengths for complex angle-ply composites from these unidirectional constituent properties have been only partially successful, as the important role of the matrix-matrix interface has not been adequately quantified. However, optical examination of failure surfaces as a function of fiber modulus and matrix microscructure allows a qualitative interpretation to be made.

† This work was supported by the U.S. Atomic Energy Commission.
‡ Presented at the Symposium on "Interfacial Bonding and Fracture in Polymeric, Metallic and Ceramic Composites" at the Univ. of California at Los Angeles, Nov. 13–15, 1972. This Symposium was jointly sponsored by the Polymer Group of So. California Section, ACS and Materials Science Department, U.C.L.A.

## I INTRODUCTION

Two classes of carbon/carbon composites consisting of either a carbon felt or carbon filament-wound substrate in a chemical-vapor-deposited (CVD) pyrocarbon matrix are being developed for reentry applications.[1,2,3] The filamentary composite offers both the greatest potential for material development as well as the greatest challenge in the understanding of its behavior. Thus, an attempt has been made to characterize and understand this composite and to obtain basic information on its micromechanics, constituent properties and fracture.[4] While only partially completed, this study has demonstrated the important role of interfaces in determining the properties of the composite and its fracture behavior.

This paper presents data concerned with the role of interfaces in a specific class of carbon/carbon composites: filamentary carbon fibers in a CVD, pyrocarbon matrix. These composites contain both fiber-matrix and matrix-matrix interfaces and thus do not fit the usual concept of fiber-reinforced composite materials. For this reason, section two presents a detailed description of this composite and will attempt to demonstrate the complexity of the overall problem. The remaining sections will present, in order, results for increasingly complex fibrous geometries in a pyrolitic carbon matrix: single fiber, strand or yarn bundle, and angle-ply filament-wound cylinders. By necessity, these arguments must become more qualitative as the complexity increases. However, the dependence of failure modes and composite properties upon the various interfaces can be illustrated.



## II CARBON FILAMENT/PYROLYTIC CARBON MATRIX COMPOSITES

An accurate picture of this carbon filament–pyrolytic carbon matrix composite is prerequisite for understanding the subsequent data and discussion. An overall view of this filament-wound, CVD composite (CVD/FW) is given in Figure 1. The filaments are Carborundum's CY2-5, a rayon-based yarn consisting of five twisted plies of approximately 480 individual fibers per ply. The filament-wound substrate was infiltrated by the temperature gradient technique from methane at 1050°C and 625 torr; additional composite fabrication details are reported elsewhere.[3,5] Figure 1A shows the outer machined surface of a cylinder with a wrap angle, defined as the angle the filaments make with the cylinder axis, of approximately 70°. Figure 1B–D are increasing magnifications under polarized light of a section taken through the thickness of this part; the plane shown is parallel to, and includes, the

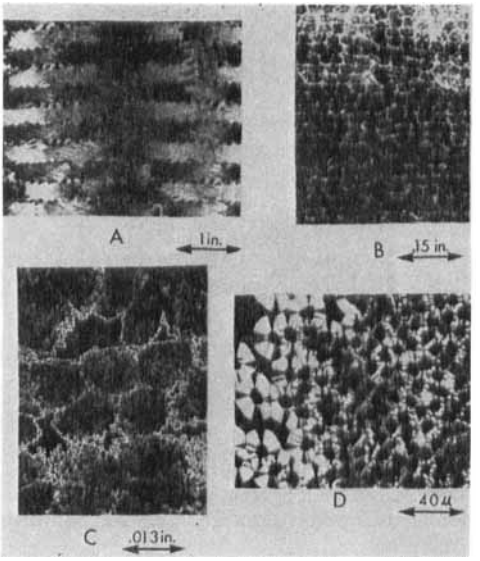


FIGURE 1 Detailed photographs of an angle-ply, filament-wound carbon/carbon composite at increasing magnification. B, C and D are polished surfaces under plane polarized light.



cylinder axis. Typical of this composite and evident in Figure 1 are: (a) the layering of the yarn and crossover voids produced by the filament-winding process (Figure 1A, B), (b) the different amounts of matrix material within and between plies (Figure 1C, D), (c) long voids aligned in the fiber direction both within and between plies (Figure 1A, cross-sections visible in 1B–D), and (d) fiber-matrix interfaces and various types of matrix-matrix interfaces (Figure 1A–D). Figure 2 presents a scanning electron micrograph of individual fiber-matrix units clearly showing the crenulated rayon-based carbon fibers, the layered pyrocarbon matrix, and matrix-matrix interfaces.

The usual idea of a matrix brings to mind a uniform, continuous, and essentially void-free material which occupies all of the available volume between the fibers. In a chemical-vapor-deposited matrix, however, deposition occurs uniformly around each individual fiber. Deposition can continue until these sheaths intersect forming a matrix-matrix interface; often several intersections will result in a closed inaccessible pore. As growth occurs only where the source gas can penetrate, the amount and extent of matrix deposition can vary depending upon the relative geometry and pore size in the substrate. The result is that the kind and number of interfaces in a CVD-deposited matrix are quite different than those associated with the usual concept of a composite material. The pyrocarbon matrix also differs in another important aspect: it is a brittle material with an ultimate failure

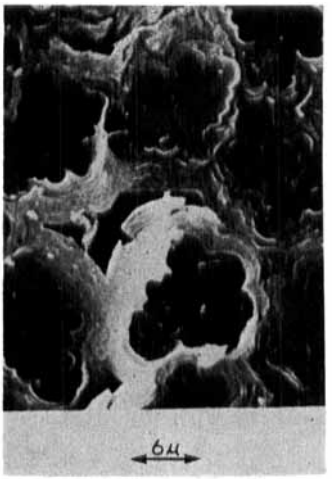


FIGURE 2 Scanning electron micrograph of individual fiber-matrix units showing crenulated, rayon-based fibers, layered pyrocarbon matrix, and matrix-matrix interfaces.



strain of 0.1 to 0.6 percent. (This value may be determined, in part, by the failure strain of the matrix-matrix interfaces.) Thus, the composite's failure strain may be governed by the matrix strain to failure.[4] This brittle nature of the pyrocarbon matrix also prevents it from fully providing those functions normally associated with a matrix material:[6] preventing a crack from propagating through the composite, providing uniform load distribution among fibers, and redistributing the load around individual fiber breaks.

Different pyrocarbon microstructures and a variety of carbon fibers exist so that a wide range of properties are possible within this class of composites.[7] Table I summarizes several of the different constituent variations. For example, the composite shown in Figure 1 consists of a turbostratic, smooth laminar matrix with high preferred orientation around a rayon-based, low-modulus, 5-ply yarn filament-wound in an angle-ply geometry. Either directly or indirectly, each of these variations will affect the nature of the interfaces within the composite and most of them cannot be investigated independently.

The complexity of the overall problem is obvious. However, in the following sections, data and observations will be presented on fiber-matrix and matrix-matrix interfaces for primarily a smooth laminar matrix microstructure as a function of polyacrylonitrile (PAN)- and rayon-based fibers of different moduli, composite heat treatment to 3000°C, and substrate geometries from single fibers to angle-ply filament-wound yarns. In particular, the low strength and load-carrying capability of the matrix-matrix interface in shear and tension will be shown to be a major factor in the determination of this composite's behavior.

TABLE I
Some constituent variations possible in carbon fiber/pyrolytic carbon matrix composites[a]

| | | |
|---|---|---|
| *Matrix* | | |
| Microstructure | Smooth laminar<br>Rough laminar<br>"Isotropic"<br>Combinations | These microstructures are produced by the different gas phase reactions occurring under different CVD conditions and are categorized by their appearance under polarized light which reflects the degree of preferred orientation of the anisotropic crystallite in the viewing direction. The anisotropy of the matrix properties can be inferred from the matrix microstructure. |
| Crystallite structure | Turbostratic → graphitic<br>$d_{002}$ : > 3.44 → 3.354Å<br>$L_c$ : 20 → > 400Å | Pyrocarbon deposited below 1500°C is classified as turbostratic. Heat-treatment above 1500°C graphitizes the material to an extent determined by the treatment parameters and microstructure. Increased anisotropy and more graphitic properties result; in particular, the interplaner shear strength is lowered. |
| *Fibers* | | |
| Precursor | Polyacrylonitrile (PAN)<br>Rayon | Affects fiber cross-section: round (PAN), crenulated (rayon). Different processing parameters also produce different changes in fiber properties upon heat treatment. |
| Modulus | High, 30–75 × $10^6$psi<br>Intermediate, 8–30 × $10^6$psi<br>Low, 4–8 × $10^6$psi | Related to the carbon fiber structure; alignment and preferred orientation of the ribbon crystallites along the fiber axis increases with increasing modulus. Thus, axial thermal expansion is inversely proportional to modulus. |
| Yarn | Fibers/ply, plies/yarn<br>Tows<br>Twist<br>Diameter, etc. | The physical appearance of filaments directly affects the nature of the filament-wound substrate, and indirectly affects the amount and distribution of matrix and matrix-matrix interfaces. |
| Substrate | Unidirectional<br>Angle-ply<br>Woven, three-dimensional | Substrate geometry and application determines subsequent stresses placed upon various interfaces in the composite. |

[a] See Ref. 7, for example, for further discussion.

## III INDIVIDUAL FIBER/MATRIX COMPOSITES

Only the fiber-matrix interface is present in the simplest composite unit: a single fiber in a pyrocarbon sheath. Unidirectional, PAN- and rayon-based fiber/matrix units were tested in axial tension to determine composite modulus as a function of matrix volume fraction. Of interest was whether

the modulus obeyed a rule-of-mixtures (ROM) relationship:

$$E_c = E_f(1 - V_m) + E_m V_m$$

where $E$ is Young's modulus and $V$ is the volume fraction, and the subscripts $c$, $f$ and $m$ refer to the composite, fiber and matrix, respectively. Implicit in the derivation of this relationship is the assumption that the strains in fiber and matrix are the same and, thus, the fiber-matrix interface is sound and provides a means for load transfer.

Simple composites to test this assumption were made by resistively heating a multifiber strand in a flowing stream of methane at a maximum observed strand temperature of 1100°C. Single fiber units, approximately 1 cm long, were extracted from the strand, about 0.2 cm at each end were bonded to grips with diphenyl cabazide, and were tested in tension to constant load on a Tecam microtensile tester. The samples were not failed and the volume fractions were determined after test from cross-sections of each sample.

The results for Whittaker-Morgan's PAN-based, Modmor II/pyrocarbon composite are shown in Figure 3.[8] The upper line represents the ROM

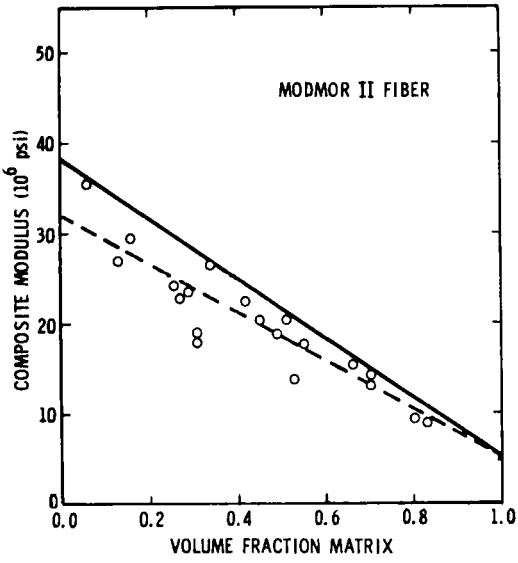


FIGURE 3 Modulus of single fiber (Modmor II) matrix units as a function of matrix volume fraction. Solid line: ROM prediction based on measured fiber modulus. Dashed line: Linear least squares fit of the data.

prediction of modulus based on a fiber modulus of $38 \times 10^6$ psi (single fibers measured on the same apparatus) and a matrix modulus of $5.0 \times 10^6$ psi. The latter value has been obtained from extrapolation in similar experiments of this kind and is consistent with values of pyrolytic carbon deposits of

similar structure.[9] The dashed line represents a linear least-squares fit of the composite data points and results in extrapolated values of $32 \times 10^6$ and $5.0 \times 10^6$ psi for the fiber and matrix moduli, respectively.

As the matrix sheath was bonded to the grips, two mechanisms are available for load transfer to the fiber: either through a sound interfacial bond or a physical Poisson's contraction of the matrix sheath upon the fiber. In the absence of any fiber-matrix interaction, the observed modulus would be that of the matrix and would increase from zero to $5 \times 10^6$ psi as $V_m$ increased to 1.0. The contraction mechanism would produce a nonlinear, concave-up stress-strain curve, but all experimental load-strain curves were linear from the origin. Thus, load transfer is occurring through interfacial bonding. The difference between the extrapolated and measured bare fiber modulus may be due to changes in fiber properties which occurred during the CVD process and/or interface cracking induced by the differences in thermal expansion between fiber and matrix upon cooling from 1100°C. Thus, the fact that all data points fall slightly below the ROM prediction may not be indicative of less-than-perfect interfacial bonding.

Similar limited data were obtained for the rayon-based Thornel 50 fibers. Experimental difficulties in extracting sound, single fiber-matrix units of adequate length from the infiltrated strand limited the range of matrix volume fractions and may have affected the precision of the data. The results are shown in Figure 4; the ROM prediction is based on a measured

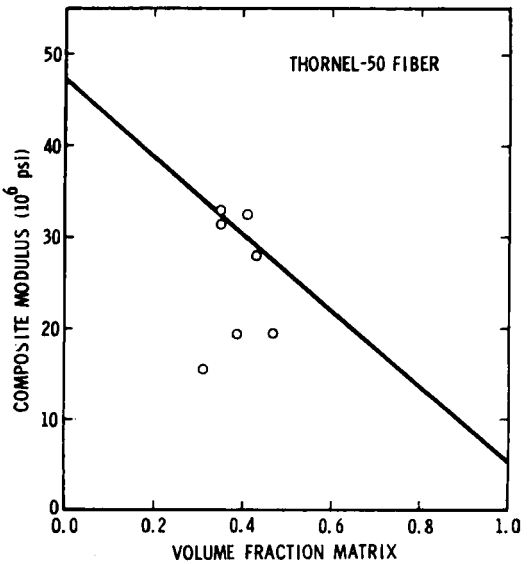


FIGURE 4 Modulus of single fiber (Thornel 50) matrix units as a function of matrix volume fraction. Solid line: ROM prediction based on measured fiber modulus.

fiber modulus of 47 × $10^6$ psi and the matrix modulus of 5 × $10^6$ psi. Again, observed load-strain curves were linear to 50–80 percent of expected ultimate strength and the samples were not failed. While the results are not conclusive, the observed moduli appear to have the ROM predictions as an upper limit. Low moduli are observed in three cases, but these moduli are still well above the < 5 × $10^6$ psi expected in the case for no reinforcement.

## IV UNIDIRECTIONAL STRAND/MATRIX COMPOSITES

The infiltrated strand, a collection of individual fiber-matrix units, forms the basic unit for the actual filament-wound composites of interest. At this level of complexity, a matrix-matrix interface is introduced by the intersection of the pyrocarbon sheaths growing about the individual fibers which comprise the strand. As was shown in the preceding section, the fiber-matrix bond is sound so both the fiber and matrix contribute to the properties of the single fiber-matrix units. The matrix-matrix interfaces between the units become important since, as seen in Figure 5, the strands are twisted slightly

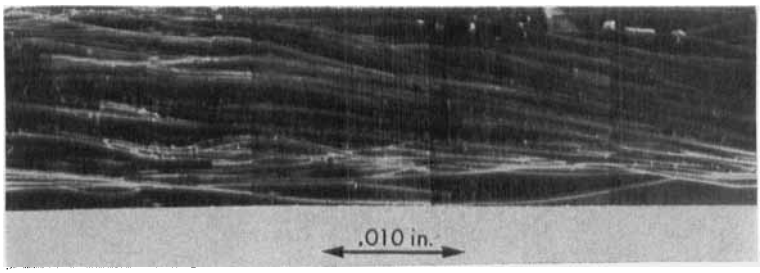


FIGURE 5 Scanning electron micrograph of an infiltrated strand.

and are not truly unidirectional. In addition, there is porosity between the fiber-matrix units to a degree dependent upon both the amount of twist and matrix volume fraction.

When an axial tensile stress is applied to the uniaxial strand composite, the twist induces a shear stress which exceeds the matrix-matrix interface shear strength well before the composite's ultimate axial tensile strength is attained. Due to this easy interface failure, the fiber-matrix units within the strand are allowed to move relative to one another. Thus, the strand composite modulus can be represented by:

$$E_s = \frac{\sigma_s}{\epsilon_s}$$

where $\sigma_s$ is the average applied stress in the composite and $\epsilon_s$ is the measured strain. $\epsilon_s$ is the sum of both the actual strain in the individual fiber-matrix units and the apparent strain resulting from rearrangement of the units after partial or complete failure of the matrix-matrix interfaces. (This rearrangement can be thought of as a lateral movement of the units to fill the porosity, thus lengthening the strand without actually straining the units.) The matrix does not maintain the relative position of the fibers with respect to one another and, thus, the composite behaves much like a rope or strand composed of individual fiber-matrix units. The end result is that the measured $\epsilon_s$ is greater than, and the resulting modulus is less than, the strain and modulus within the units themselves. Note that as matrix volume fraction increases, this relative movement and this additional strain would be expected to decrease.

Carborundum's CY2-5 and Union Carbide's Thornel 16, Thornel 25 and Thornel 50, rayon-based yarns with different moduli, were used to evaluate the properties of these strand-matrix composites. The strands were infiltrated by resistively heating them at 1100°C in a stream of methane at 625 torr for different lengths of time to obtain the different matrix volume fractions. These strands were bonded with epoxy to metal tabs with a one inch gauge length and tested in tension at a crosshead speed of 0.05 cm/min. The load-deflection curves for high matrix volume fraction composites were linear from start of test through failure; strands with little or no matrix exhibited linear behavior only after an initial concave-up portion at low loads. Volume fractions for each specimen were obtained from both liquid displacement measurements and microphotographs of sections of the strand adjacent to the test section.



The observed composite moduli for infiltrated Thornel 50 strands are shown in Figure 6; each data point is the average of four tests. The line drawn represents a linear least square fit of the data which includes the measured modulus of an as-received, bare strand ($V_m = 0$). Also shown in the figure is the rule-of-mixtures prediction for the single fiber-matrix units derived in the preceding section. The difference between the two results is directly attributable to the weakness of the matrix-matrix interface. the twist of the fibers, and the inherent porosity as just discussed. The agreement between the composite and bare strand values is consistent with the concept of strandlike behavior for this particular strand composite.

Figure 7 shows the observed composite moduli for the four different strand composites investigated. In each case, the observed moduli are considerably less than a ROM prediction for the individual fiber-matrix units and the experimental values are consistent with measured moduli for bare strands. Table II presents single fiber and bare strand strengths and moduli for these four carbon fibers.

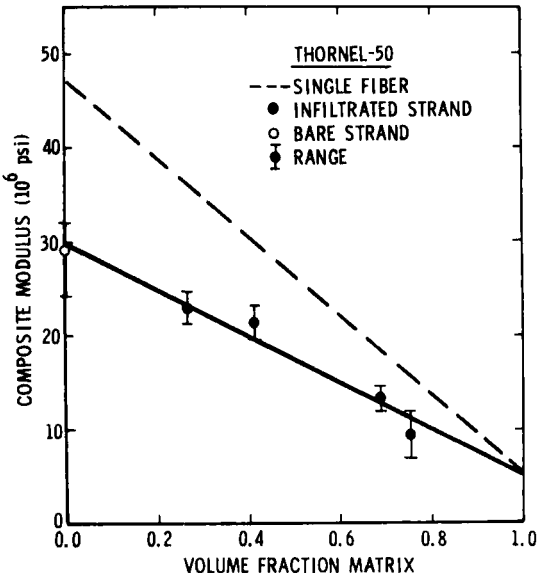


FIGURE 6 Observed composite moduli for infiltrated Thornal 50 strands as a function of matrix volume fraction. Dashed line is ROM prediction in Figure 4. Each data point is the average of four tests.

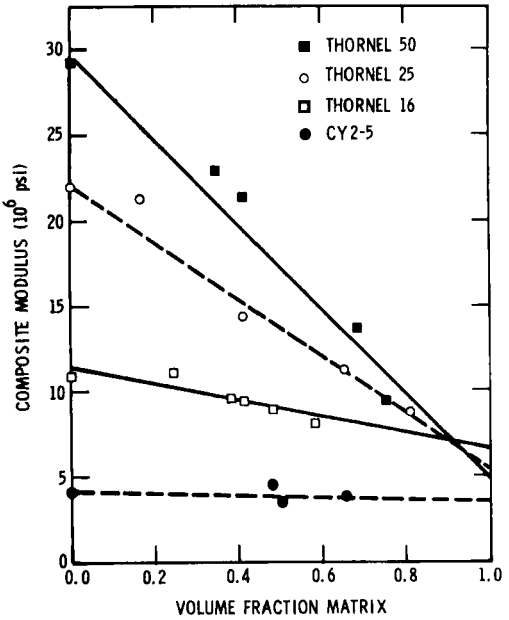


FIGURE 7 Observed composite moduli for four infiltrated strands as a function of fiber and matrix volume fraction. Each data point is the average of four tests.

TABLE II
Properties of carbon fibers tested[a]

| Fiber | Single fiber | | Bare strand | |
|---|---|---|---|---|
| | Strength ($10^3$psi) | Modulus ($10^6$psi) | Strength ($10^3$psi) | Modulus ($10^6$psi) |
| Thornel 50 | 348 ± 31 | 45.9 ± 3.7 | 112 ± 9.8 | 28.8 ± 2.5 |
| Thornel 25 | 249 ± 31 | 27.4 ± 1.6 | 106 ± 13.0 | 21.6 ± 2.7 |
| Thornel 16 | 166 ± 22 | 14.0 ± 0.7 | 96.7 ± 2.0 | 10.8 ± 0.2 |
| CY2-5 | 131 ± 41 | 4.7 ± 0.7 | 57.0 ± 16.7 | 4.13 ± 0.43 |

[a] 90 percent confidence intervals.

Strength arguments are more complicated and, while quantitative conclusions cannot be made due to scatter in the data, limited results indicate the same relationships are valid. Figure 8 shows composite strengths for infiltrated Thornel 50 strands. The precision exhibited by this data set must be

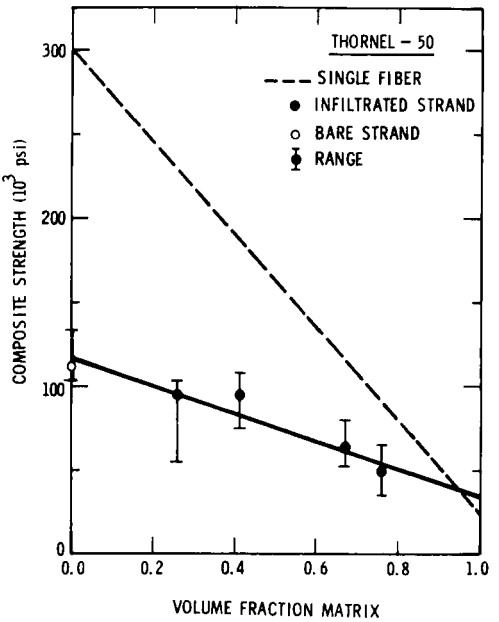


FIGURE 8 Observed composite strengths for infiltrated Thornel 50 strands as a function of matrix volume fraction. Dashed line is ROM prediction based on single fiber strengths.

considered to be fortuitous since, in this case, the strain-to-failure of fiber and matrix are essentially the same. The single fiber-matrix ROM prediction was assumed from measured single fiber strengths (Table II) and a reported 20,000 psi matrix strength.[9] Again the results show that the composite data fall well below the individual unit predictions but are consistent with the ultimate strength of a bare strand.

The easy failure of the matrix-matrix interface does not allow a mechanism by which the applied load can be equally distributed between the individual units. Nor, in the case of individual unit failures, can the load be re-distributed either within the same fiber-matrix unit away from the failure location, or among adjacent units in the vicinity of the fracture. As these weak interfaces fail, the stress distribution (i.e., the number of fiber-matrix units at a given stress as a function of stress) becomes very broad. The failure of some number of highly-stressed units then results in composite failure since load redistribution is not possible. This situation simply reflects the fact that a strand of fibers (or units) will exhibit a lower strength than a single fiber (or unit).[6]

Thus, the potential properties of carbon fiber-pyrocarbon matrix composites are more appropriately determined by the strand properties given in Table II and not by the more attractive single fiber properties. These results are the direct result of the pyrocarbon matrix not providing the usual matrix functions as discussed in Section II.



## V ANGLE-PLY, FILAMENT-WOUND COMPOSITES

At this level of complexity, additional matrix-matrix interfaces are introduced to the composite. As before, these interfaces are formed by the intersection of pyrocarbon sheaths growing at equal rates around the filament strands that have been arranged by the filament winding operation. The winding process produces two kinds of relative filament arrangements and gives rise to both interlaminar and intralaminar matrix-matrix interfaces between infiltrated strands. These strand-strand interfaces are shown schematically in Figure 9; this figure can be compared with the photographic description given in Figures 1 and 2. While the nature of these interfaces are basically the same (i.e., pyrocarbon-pyrocarbon), their geometry and, hence, load-bearing capability are different. This substrate geometry depends upon wrap angle, filament tension during winding, use of adhesive during winding, and the strand's physical description with respect to twist, number of plies, individual fibers, etc.

With reference to Figure 9, a circumferentially-wrapped cylinder (wrap angle = 90°) tested in hoop (by internal pressure) or axial tension produces stresses parallel to ($\sigma_L$) and transverse to ($\sigma_T$) the infiltrated strand, respectively. Theoretically, there are no shear stresses acting upon the strand-strand interfaces; however, some shear stress probably exists due to strand twist and winding irregularities.

At wrap angles other than 0 or 90°, an applied axial or hoop stress also results in a shear stress ($\sigma_S$) in addition to $\sigma_L$ and $\sigma_T$. The actual shear

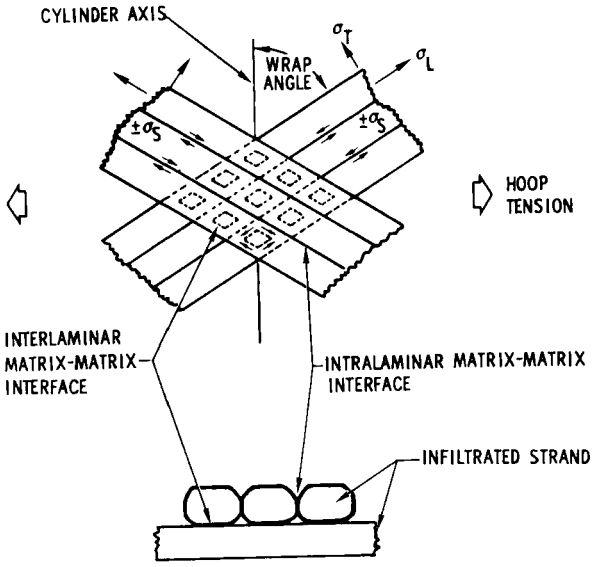


FIGURE 9 Schematic representation of an angle-ply, filament-wound composite showing different strand-strand interfaces and distribution of an applied hoop stress.



strengths of the interlaminar and intralaminar strand-strand interfaces are nherently low thus providing preferred failure surfaces which, to a large extent, determine the composite's failure mechanism and strength. A SEM photograph of the failure surface of an angle-ply cylinder (CY2-5 filaments at a wrap angle of 70°) tested by internal pressure is shown in Figure 10. Clearly evident in Figure 10A are the infiltrated strands, the angle-ply nature of the composite, interlaminar and intralaminar shear failure surfaces, and axial tensile failure surface of the strands. The failed interlaminar interface is shown with increasing magnification in Figures 10B–D.

Thus, composite failure behavior is determined by (1) the distribution of the applied stress, which depends upon direction of applied load, wrap angle, fiber and matrix moduli, and interface geometry, and (2) upon the relative tensile and shear strengths of the constituents and interfaces present. These relative strengths can only be qualitatively described from observations of the fracture surfaces since the stresses cannot be modeled in a more easily defined, less complex system. However, the effects of changes in wrap angle, fiber modulus and matrix properties before and after heat treatment upon composite behavior can be examined.

The samples examined were cylindrical and were fabricated by filament winding on three inch diameter graphite mandrels and infiltrated by standard methods.[10] The samples were tested in either axial tension or by the applica-

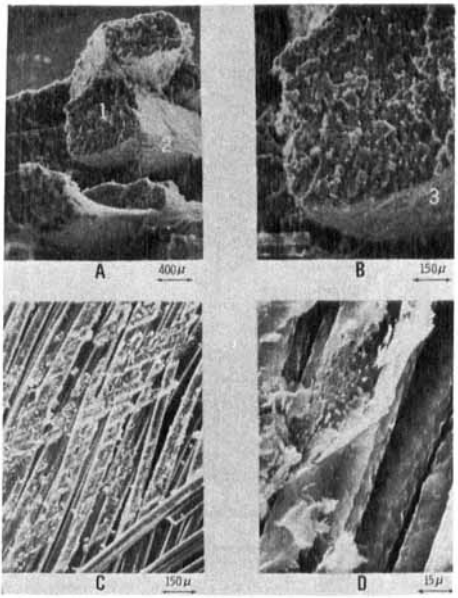


FIGURE 10 Scanning electron micrographs of an angle-ply, filament-wound composite. A1: Axial tensile strand failure surface; A2: intralaminar Interlaminar matrix-matrix and shear failure; C, D: Increased magnifications of interlaminar shear failure; B3.

tion of internal pressure (burst test). The latter was assumed to result in a uniform hoop stress since the internal radius to wall thickness (0.125 in.) ratio was greater than ten. Thus, depending upon wrap angle and type of test, the load could be applied anywhere from 0 to 90° to the filament direction.[4]

The effects of wrap angle and/or direction of applied stress were examined on heat-treated, CY2-5 cylinders. The fracture behavior and the observed stress-strain curves are illustrated in Figures 11 and 12, respectively. The burst test applied a hoop stress at $\pm 20°$ to the strand direction and the axial fracture indicates that the predominant mode was strand tensile failure. However, the nonlinear stress-strain curve suggests that interlaminar shear failures occurred prior to ultimate failure. By comparison, the axial tensile test increased the applied stress transverse to the strands and failure occurred along the strand-strand interfaces as seen by the failure surface which parallels the wrap angle. Thus, the various strengths (axial infiltrated strand, transverse matrix-matrix, etc.) were the same in each case, but the observed failure mode depended upon the distribution of the applied stress as determined by wrap angle and test direction. Figure 12 also presents data for other wrap angles and load directions from 0 to 90°.[4] The different matrix-matrix interfaces and strengths manifest themselves in the nonlinear stress-

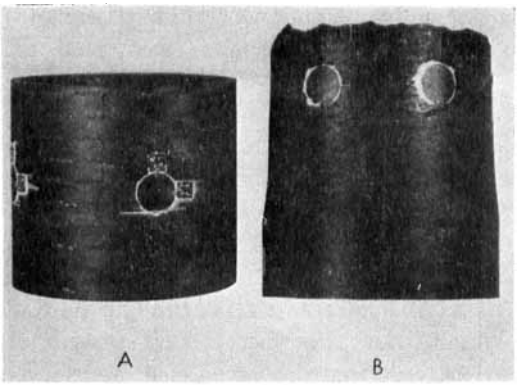


FIGURE 11 Failure modes in a 70°, filament-wound, CY2-5 cylinder failed under hoop (A) and axial (B) tension.



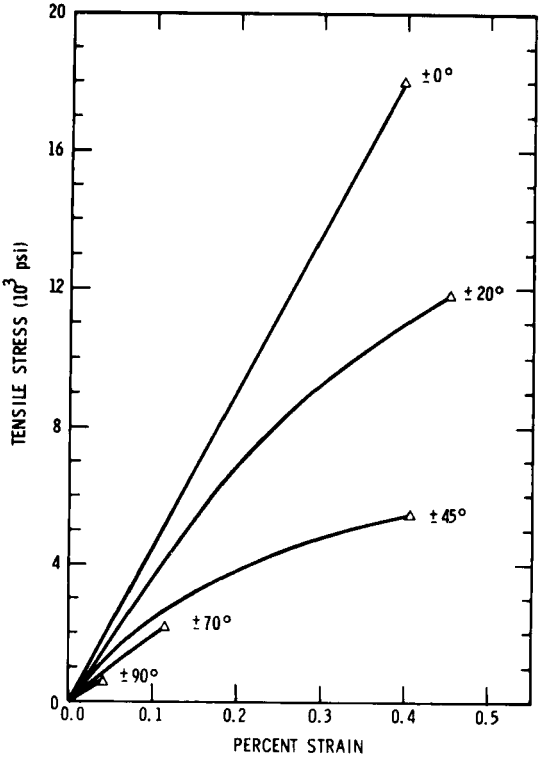


FIGURE 12 Observed stress-strain curves and tensile strengths for filament-wound CY2-5 cylinders. Tensile stress applied to the strand direction at the angle shown. (Adapted from data presented in Ref. 4).

strain curves and the sharp reduction of ultimate strength and strain with increasing angle from the infiltrated strand axis. Note that the $\pm 0^\circ$ and $\pm 90^\circ$ tests are indicative of the axial strand and matrix-matrix tensile strengths, respectively.

Changes in fiber moduli and, in turn, infiltrated strand strengths and moduli also affect the fracture behavior. The different fracture in composites made with low modulus (Carborundum's GY2-1, $5 \times 10^6$ psi) and high modulus (Hercules HMG-50, $50 \times 10^6$ psi) filaments and burst by internal pressure are shown in Figures 13A and C. The fracture changes from one dominated by axial infiltrated strand strength (GY2-1) to one dominated by the strand-strand interface shear strength (HMG-50). This change is due to the fact that the increased strand tensile strength is not accompanied by an increased strand-strand interface strength. In fact, the latter may actually be weakened by matrix cracking induced by a difference in thermal expansion between the axial and transverse directions within the strand upon cooling from deposition temperatures. These thermal stresses are proportional to the thermal expansion anisotropy in the fiber-matrix unit. The results are complicated by differences in yarn configuration as discussed previously, but tests with many high modulus filaments have shown similar strand-strand interface failures.

Finally, the effect of heat treatment upon the failure mode is considered. This procedure graphitizes the matrix to an extent depending upon the heat treatment parameters and the matrix character. The interlaminar shear strength, and thus the strand-strand interface strengths, decrease with increased degree of graphitization. This effect is shown in Figures 13A and B which illustrates two failure modes for Carborundum's GY2-1 tested in the as-deposited (1100°C) and heat-treated (3000°C, 2 hrs) condition. The

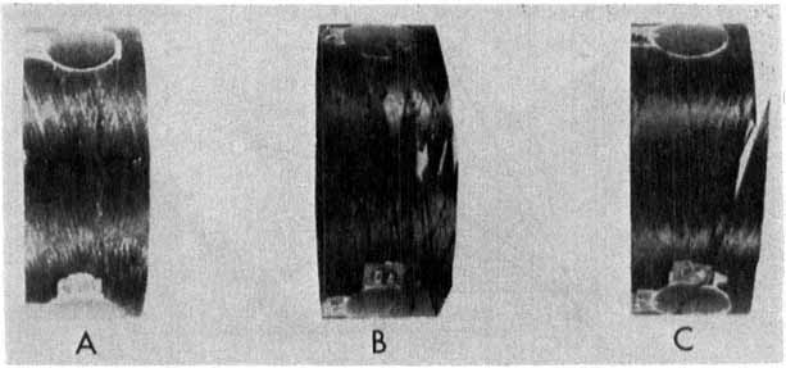


FIGURE 13 Observed failure modes under hoop tension in $\pm 70^\circ$, filament-wound cylinders. Carborundum's GY2-1 fiber ($5 \times 10^6$ psi modulus): as-deposited (A) and composite heat-treated (B) at 3000°C, 2 hrs. Hercules HMG-50 fiber ($50 \times 10^6$ psi modulus): as-deposited (C).

dramatic change in fracture was due to the decrease in the strand-strand interfacial bond strengths in shear and/or transverse tension relative to the strand tensile strength upon graphitization.

Therefore, for a given wrap angle and direction of applied load, any factor which tends to increase the ratio of infiltrated strand axial tensile strength to the strand-strand interfacial shear and transverse tensile strengths will tend to drive the failure mechanism toward the strand-strand interface mode and usually a decrease in composite strength. The effects of fiber modulus and heat treatment upon this ratio and resulting change in failure mode have been examined. Some of the other factors which affect the distribution of the applied stress and the various tensile, compressive and shear strengths within this complex composite have been discussed.

## VI SUMMARY

There are three classes of interfaces which are important in determining the properties of carbon filament/pyrocarbon matrix composites. These classes have been examined in successive sections and are:

a) the fiber-matrix interface

b) the matrix-matrix interface within an infiltrated strand

c) the intralaminar and interlaminar matrix-matrix interfaces between infiltrated strands.

The fiber-matrix interface has been shown to be adequate for load transfer and to allow reinforcement if a difference in modulus exists between fiber and matrix. The matrix-matrix interface within an infiltrated strand limits the axial strand properties to values below those observed for the single fiber-matrix units. The low strength strand-strand matrix interfaces effectively determine how the infiltrated strand properties will be utilized in a complex composite structure. Both classes of matrix-matrix interfaces are not present in the more conventional description of a fiber-reinforced composite material (e.g., carbon/epoxy or carbon/phenolic). These interfaces effectively limit composite properties to values well below the potential offered by the constituent properties and provide a complexity which to now has not been amenable to quantitative stress analysis and prediction.

### References

1. H. M. Stoller, *et al.*, Summary of Papers of the Tenth Biennial Conference on Carbon, Paper FC-57 (Defense Ceramic Information Center, Columbus, Ohio, 1971).
2. H. W. Schmitt, Summary of Papers of the Tenth Biennial Conference on Carbon, Paper FC-57A (Defense Ceramic Information Center, Columbus, Ohio, 1971).

3. H. M. Stoller and E. R. Frye, Symposium on Advanced Materials: Composites and Carbon, 165–172 (American Ceramic Society, Columbus, Ohio, 1971).
4. T. R. Guess, B. L. Butler and J. D. Theis, Symposium on Advanced Materials: Composites and Carbon, 195–203 (American Ceramic Society, Columbus, Ohio, 1971); also as SC-DR-710192, March 1971.
5. J. D. Theis, Proceedings of the Third International Chemical Vapor Deposition Conference, American Nuclear Society, Salt Lake City, 1972.
6. A. Kelly, *Strong Solids* (Oxford University Press, London, 1966). Chapter 5.
7. H. M. Stoller, *et al.*, chapter in *Fiber Composites: State of the Art*, a book to be published from the Fall Meeting of the Metallurgical Society of the AIME, Detroit, Michigan, 1971.
8. B. L. Butler and J. C. Tidmore, Summary of Papers of the Tenth Biennial Conference on Carbon, Paper FC-31 (Defense Ceramic Information Center, Columbus, Ohio, 1971).
9. J. L. Kaae, *Carbon* **9**, No. 3, 291–300 (1971).
10. E. R. Frye and R. M. Curlee, Proceeding of the Fourth National SAMPE Technical Conference: Non Metallic Material Selection, Application and Environmental Effects, p. 473, October 1972.